

Surface Inspection of the MERIT Primary Containment Chamber

*Van B. Graves
Oak Ridge National Laboratory
December 29, 2011*

1.0 Background

The Mercury Intense Target (MERIT) Experiment was conducted at CERN in the fall of 2007. It successfully demonstrated the feasibility of using a free-stream mercury jet as a target in a Neutrino Factory or Muon Collider facility.¹ This targetry concept continues to be developed in several areas, including magnet design, shielding and cooling, and mercury handling. Subsequent to the MERIT Experiment, an analysis was performed which suggested that high-velocity mercury droplets ejected from a jet by impact from a proton beam could cause surface damage to a stainless steel container in close proximity to the interaction region.² Some of the results of this simulation are shown in Figure 1. Because of this analysis and the ramifications it could have for future designs, it was felt that inspection of the MERIT jet primary containment vessel was warranted. This note summarizes the inspection results.

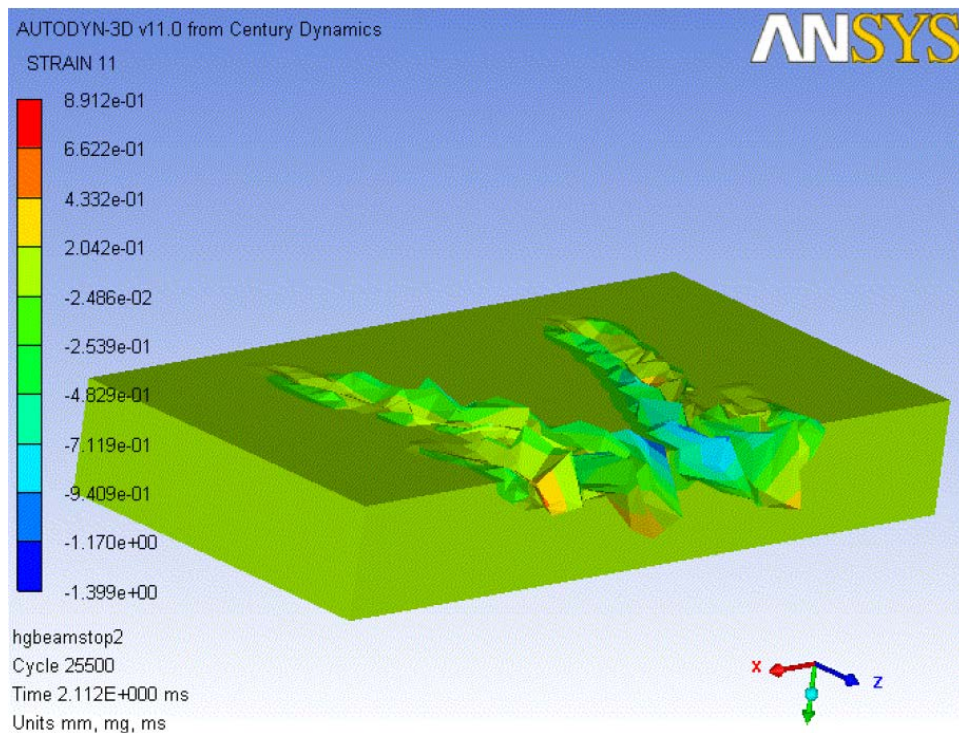


Figure 1. Simulation results showing surface damage from impact of high-velocity mercury droplets

2.0 MERIT Chamber Design

The MERIT mercury jet delivery system produced a nominal 1 cm dia., 20 m/s jet of mercury which was contained within a 15 T magnetic field. CERN required that the mercury system not be opened while on site, and the design had to provide primary and secondary mercury containment. Shown in Figure 2, the primary hardware components in the MERIT Experiment were the mercury system, the pulsed solenoid that provided the magnetic field, and the optical diagnostics system which captured the jet/beam interaction via high-speed photography.

In the MERIT Experiment, a total of 239 jet/beam interactions took place; of those, 203 included some level of constraining magnetic field and the remaining jets were unconstrained. Due to the shadow photography techniques required, measuring transverse droplet velocities incurred a large degree of uncertainty, but in general the MERIT droplet velocities were less than 80 m/s.³

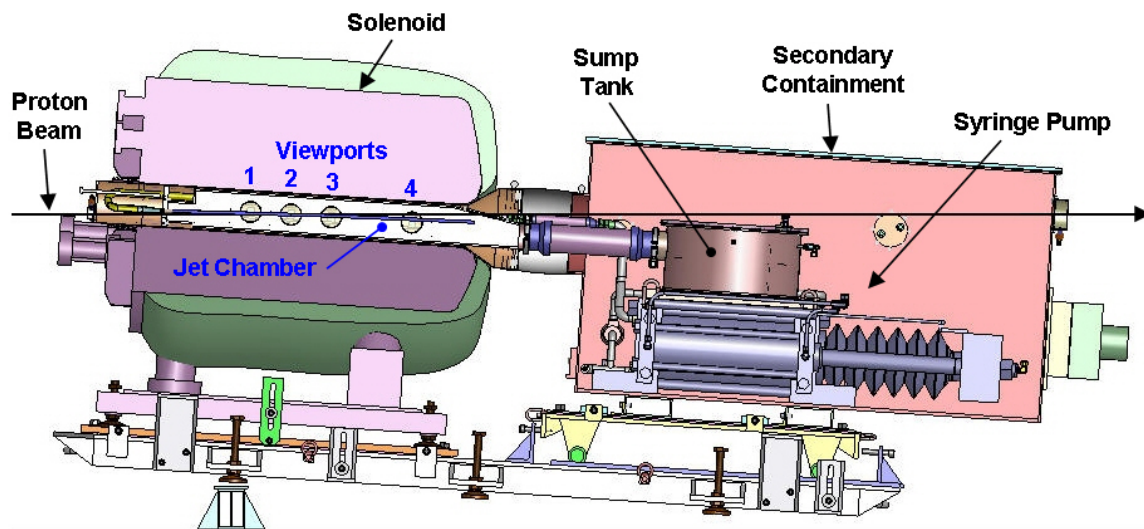


Figure 2. MERIT Experiment configuration.

The primary containment chamber which housed the mercury jet contained four optical viewports which allowed viewing of the jet; they were located such that the center of the jet/beam interaction occurred in the center of viewport #2.

Figure 3 shows a vertical cross section of the portion of the mercury system that resided inside the bore of the magnet. The circular secondary container fit within the 6" diameter magnet bore, and the rectangular primary container had an interior width of 1.4" to accommodate the 1 cm diameter jet. With the exception of the sapphire viewports, the optical diagnostic components were located outside the primary containment and were not mercury-wetted.

The primary containment chamber was fabricated from SS 316L plates. The exterior surfaces of the plates were machined to final external dimensions, but since at the time there was no perceived need to machine the interior surfaces, no surface finish requirements were imposed, and they were left with their original mill finish.

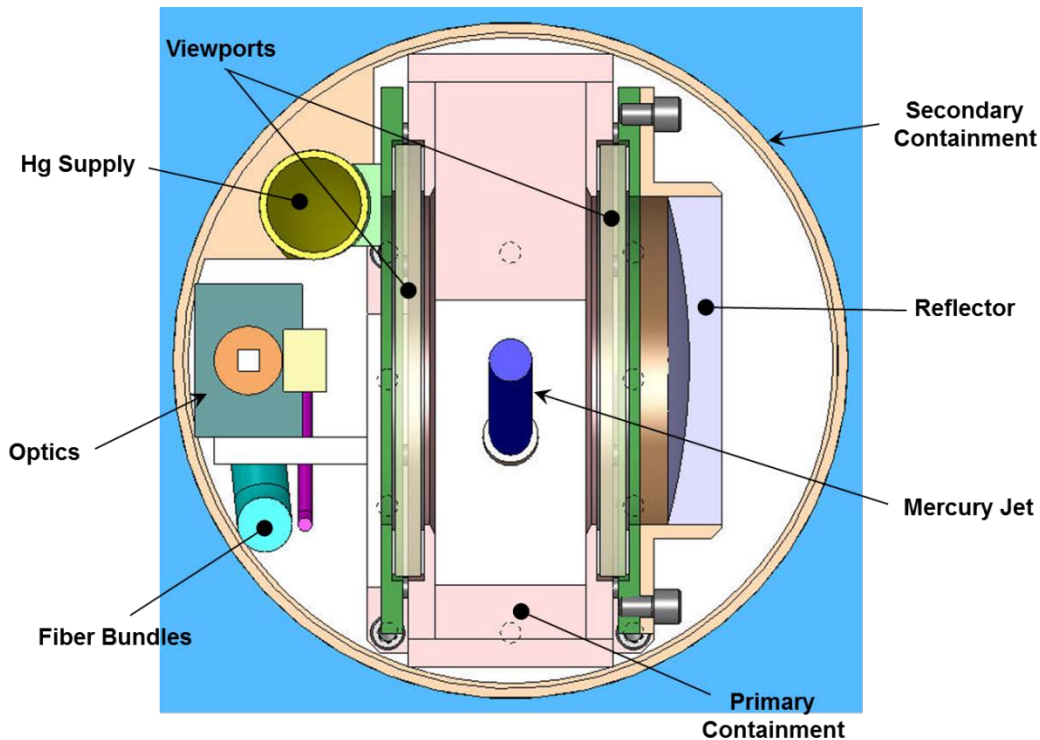


Figure 3. MERIT vertical section as viewed from downstream.

3.0 Chamber Inspection

At the conclusion of the experiment, the MERIT mercury equipment remained at CERN for several months to allow sufficient radiation decay of the mercury and the equipment. It was then transported back to ORNL in 2009 for final disposition. In 2010 the residual mercury was drained from the system, and the syringe pump equipment was disposed of. By that time, the surface pitting concern had been raised, so it was decided that the primary containment chamber should be kept for further inspection. This inspection was performed in two phases: one was a series of photographs, and the other was an actual surface profile measurement.

3.1 Photographic Inspection

Photographs of the MERIT primary containment chamber were taken in September 2010.⁴ The rectangular jet chamber was left intact, so all photographs were taken through the viewports to see the opposite interior surfaces around the port openings, as shown in Figure 4.

Figure 5 shows some representative photographs taken around viewport #2. These photographs show a surface texture which appears “rough,” and that texture could actually be felt by hand. When looking at the surfaces by eye, there was no indication of any changes in texture or surface pitting near any of the viewports, and the photographs seemed to bear this out.

To the personnel involved in the photographic inspection, who could directly view the surfaces, it was clear that there was a consistent surface finish throughout the entire chamber, which indicated that no significant surface damage had occurred during the experiment. However, this was not quite as obvious when the results were presented in Powerpoint slides since the photographs showed a textured surface

around each viewport. This led to a request to try another measurement technique that might better quantify the surface imperfections.



Figure 4. Setup for acquiring containment photographs.

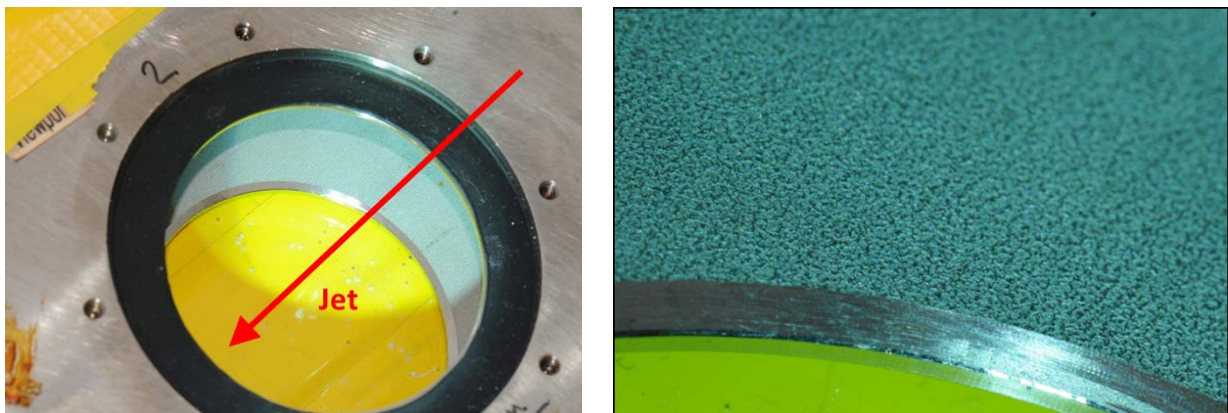


Figure 5. Viewport 2 close-up surface photos.

3.2 Surface Profile Measurement

In October 2011, measurements of the primary containment chamber were made with a Zeiss Handysurf E-35A, a portable device used to measure surface profiles for quantification of surface roughness based on national and international standards.⁵ Figure 6 shows an image of the Handysurf.



Figure 6. Zeiss Handysurf E-35A.

The instrument incorporates a 5 μ m-diameter tip on a moving stylus which supports a linear traversing length of up to 12.5 mm at a speed of 0.6 mm/s. Its stated measuring ranges are 40/160 μ m with a resolution of 0.02 μ m.

3.2.1 Reference Scans

In preparation for the measurement of the MERIT surfaces, it was desired to gain experience with the Handysurf data collection sequence by scanning the surface of some known specimens. ORNL's Spallation Neutron Source (SNS) Project has had a mercury target development program in place for several years and has performed numerous studies related to cavitation-induced surface pitting. In one such study, specimens were placed within a Split-Hopkinson Pressure Bar apparatus and subjected to varying numbers of pressure cycles, some up to 10⁶. These cycles produced surface textures with varying degrees of pitting, as shown in Figure 7. In all cases, the specimens had quantified surface finishes prior to the experiment.

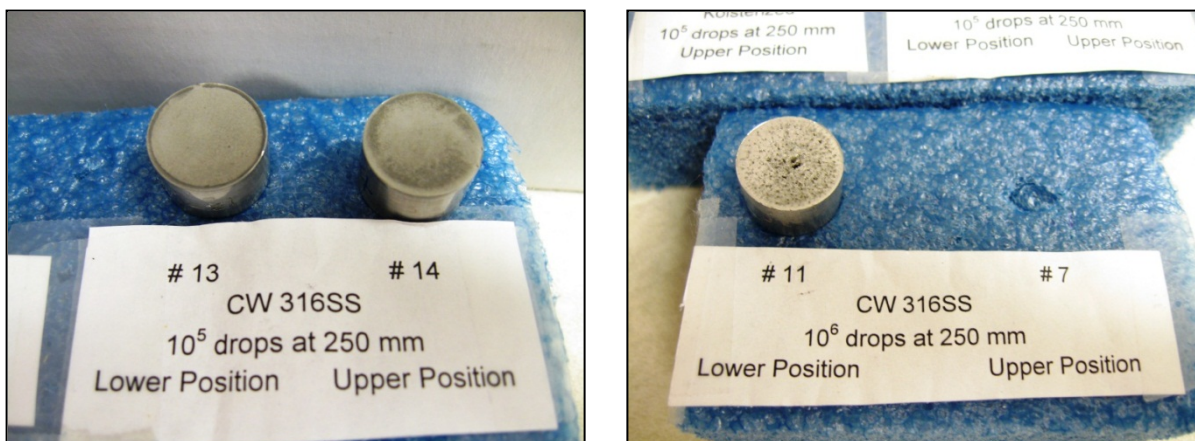


Figure 7. SNS cavitation study samples.

The Handysurf was used on four of the SNS samples, obtaining 7500 readings over an 8-mm sample length. The Handysurf software provide two separate plots for each scan, one giving an actual profile curve, and the other a roughness curve, which is the deviation from a least-squares fit through the profile data. In Figure 8, the measurement results of specimen 11 can be seen. Comparing the graphs

with the photograph in Figure 7, several of the large surface pits visible to the eye can be identified in the profile and roughness curves.

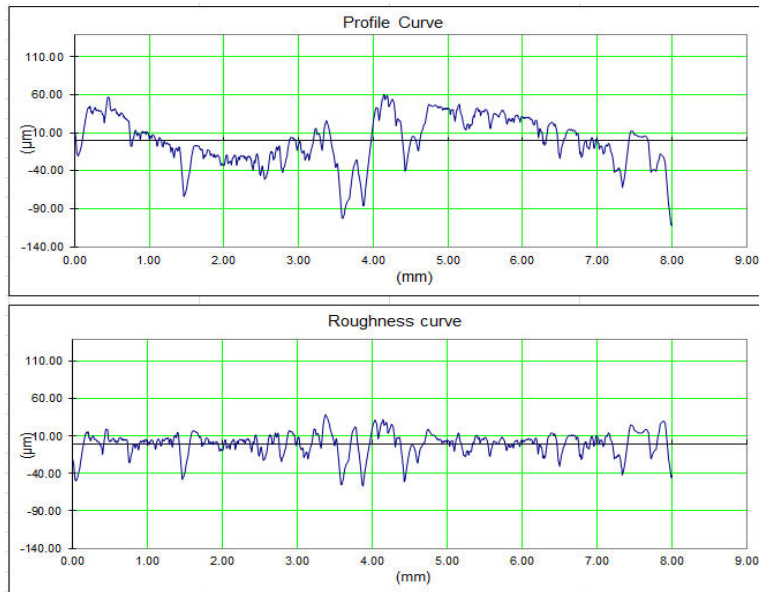


Figure 8. Surface scan results of SNS specimen 11.

Figure 9 shows the results for specimen 14, which also had some visible surface damage. Comparing the vertical scales in Figures 8 and 9, it is noted the surface profile in sample 11 had a range of approximately 150 μm , whereas in the case of sample 14, the range was only 15 μm . It is also noted that while the surface irregularities in these samples are known to come from pits, it is difficult to distinguish actual pits in the curves.

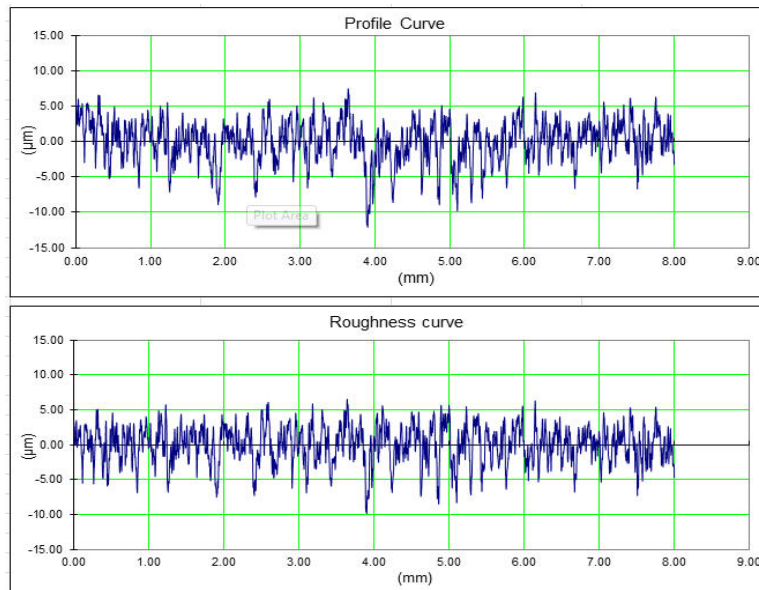


Figure 9. Surface scan results of SNS specimen 14.

In the case of specimen 14, the roughness curve is similar to the profile curve due to the relatively flat overall surface geometry and does not offer any additional insight to the discussion. This was the case for most other scans, and therefore in subsequent figures, only the surface profile curves are presented.

3.2.2 MERIT Scans

Figure 7 shows the MERIT primary jet containment chamber being uncovered for the inspection by the Handysurf. Viewports 1-3 are shown, with viewport 1 at the bottom of the image. Both exterior and interior scans were made with the device; the exterior scans were on the exposed surface shown in the figure, and the interior scans were on the bottom interior surface.



Figure 10. MERIT primary containment chamber.

A map of the scans performed is shown in Figure 8. In this figure, the viewports are sequentially number right-to-left. All the viewport scans are labeled Px_yy, where x is the port number, and yy is the scan number. Each viewport was scanned in eight areas, and the direction and approximate location of each scan being shown in the figure.

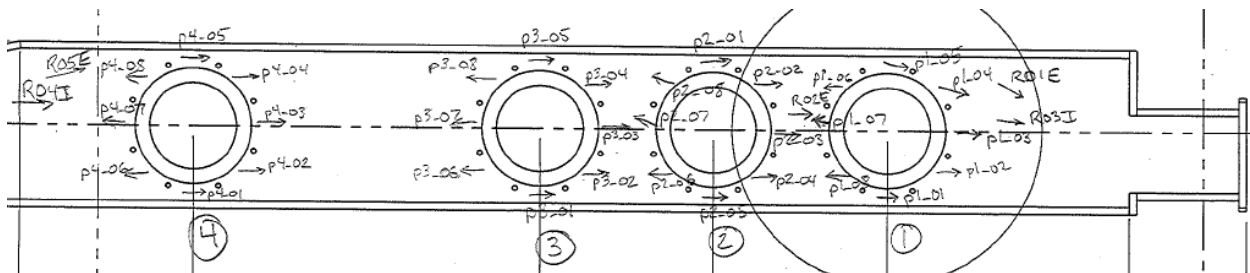


Figure 11. Scan map.

In addition, some random scans were performed in areas that should not have been affected by potentially pit-inducing droplets, as well as some scans on the exterior of the chamber for reference. These random scans are labeled RxxI or RxxE, where xx is the scan number, and I and E represent an

interior or exterior surface. Figure 9 shows representative photographs of the Handysurf as it was used during the process.

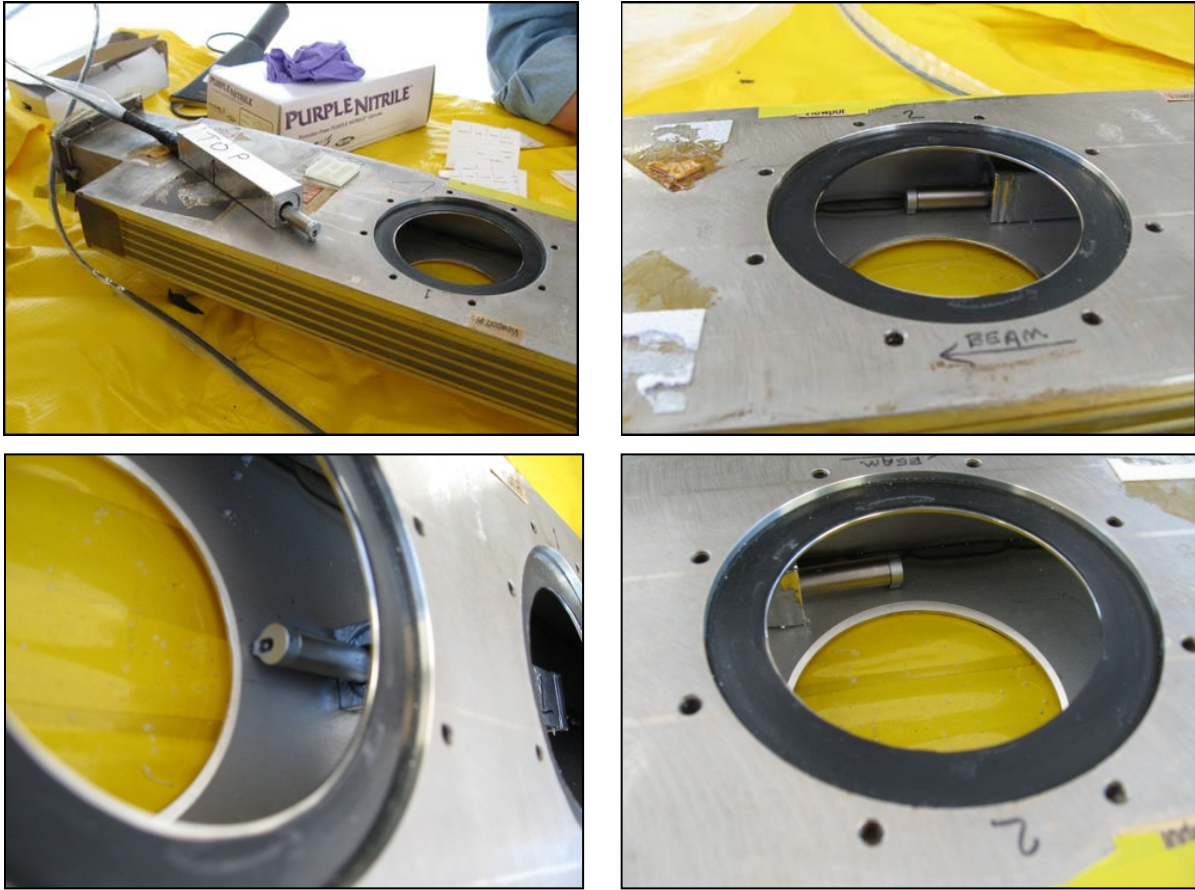


Figure 12. Handysurf measurement operations.

All the scans taken of the MERIT jet primary containment chamber are included in the Appendix. Of the most interest were the scans performed around viewport #2, which was centered on the jet/beam interaction location. Of the eight scans performed around viewport #2, scans 3 and 7 were along the beam axis and would be the most likely scans to show indications of surface damage. The profile curves produced from these scans are shown in Figures 13 and 14.

Comparing these profile curves with the photographs of viewport #2 shown in Figure 5, the apparent texture in the photographs can be observed in the scan data. It is also noted that the two curves are similar in that their deviation ranges are between $\pm 10 \mu\text{m}$, which indicates the same overall surface condition. A review of the other viewport 2 scans in the Appendix reveals very similar surface profile curves.

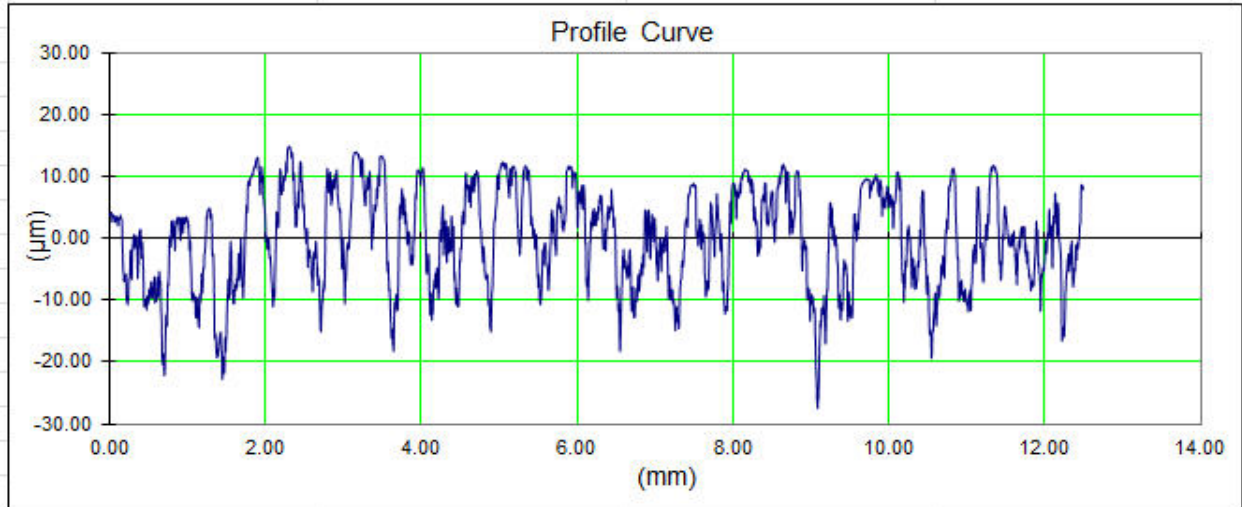


Figure 13. Scan P2_03 profile.

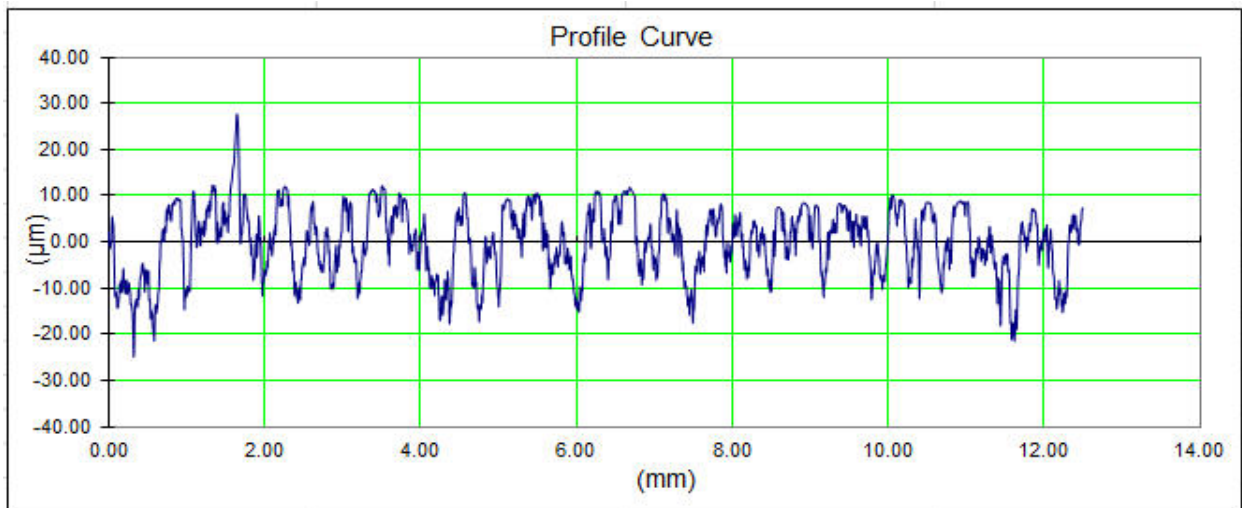


Figure 14. Scan P2_07 profile.

4.0 Discussion

A more interesting observation can be made when the viewport #2 scans are compared to other locations on the same interior surface, which can be seen in Figure 15. From the scan map shown in Figure 11, it is seen that the R04 scan was taken downstream of viewport #4, well outside the area where any kind of damage-inducing droplets would be expected. It is noteworthy that no distinguishable differences exist between the scans around viewport #2 and this downstream location.

As another point of comparison, the profile from measuring an exterior surface of the MERIT chamber is shown in Figure 16. This surface was machined to final dimension, and the improved flatness of the surface can be seen in the figure. It is noted that even this machined surface shows local deviations of 10-20 μm , so even if mercury droplets could have impacted and damaged this surface, it would be

difficult to distinguish from surface imperfections. So the relative roughness of the interior surface is not surprising, considering it had no machining or other surface preparation prior to fabrication.

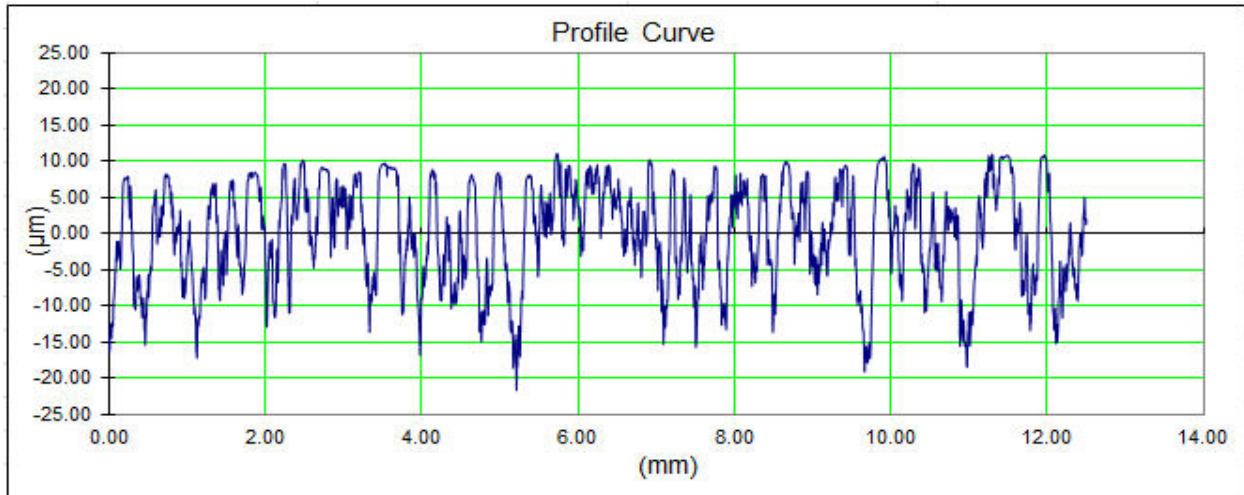


Figure 15. Scan R04 profile (interior surface).

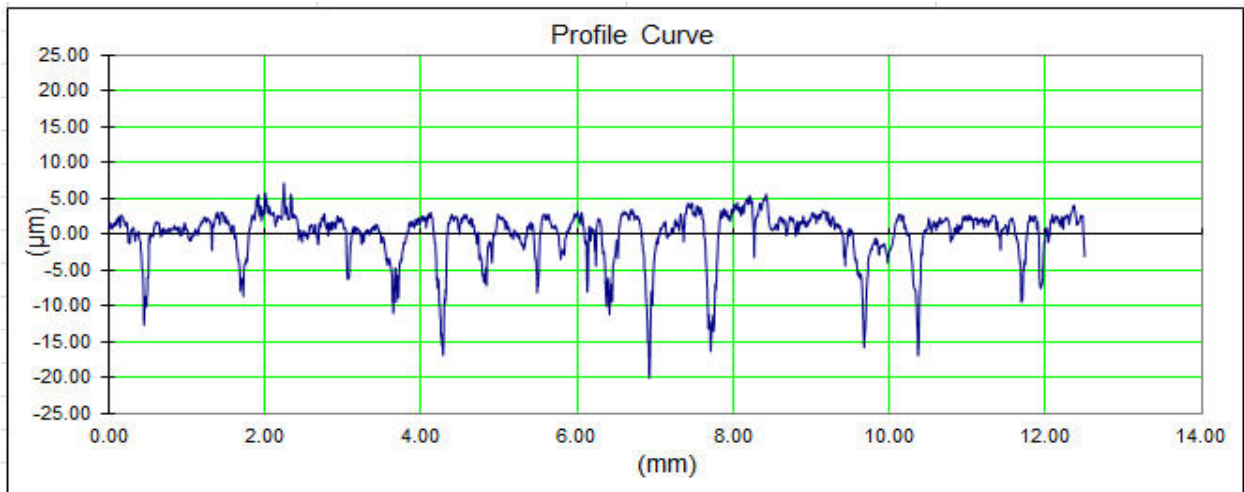


Figure 16. Scan R01 profile (exterior surface).

After review of all the scan data, there is no supporting evidence that the surfaces around any of the viewports, #2 in particular, show any differences in surface profile that would indicate damage caused by mercury droplets ejected from the jet. The expected size of any damage-induced pits is very small compared to the overall surface roughness of the MERIT jet containment chamber, such that individual pits are indistinguishable. It is also noted that an experiment designed to more precisely measure surface damage would require specially-prepared test specimens with known surface conditions prior to use in the experiment.

5.0 Appendix

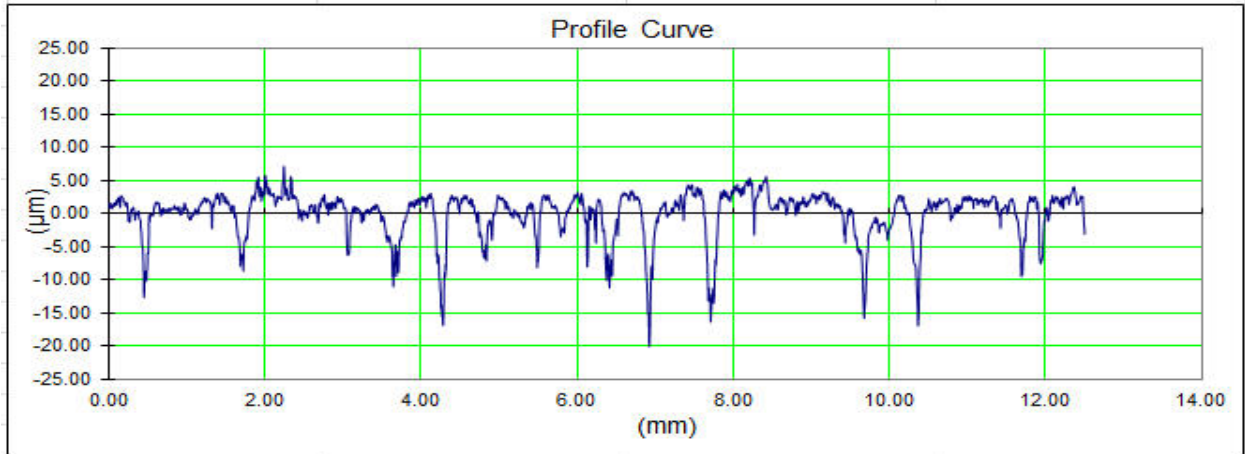


Figure 17. Scan R01 profile (exterior surface).

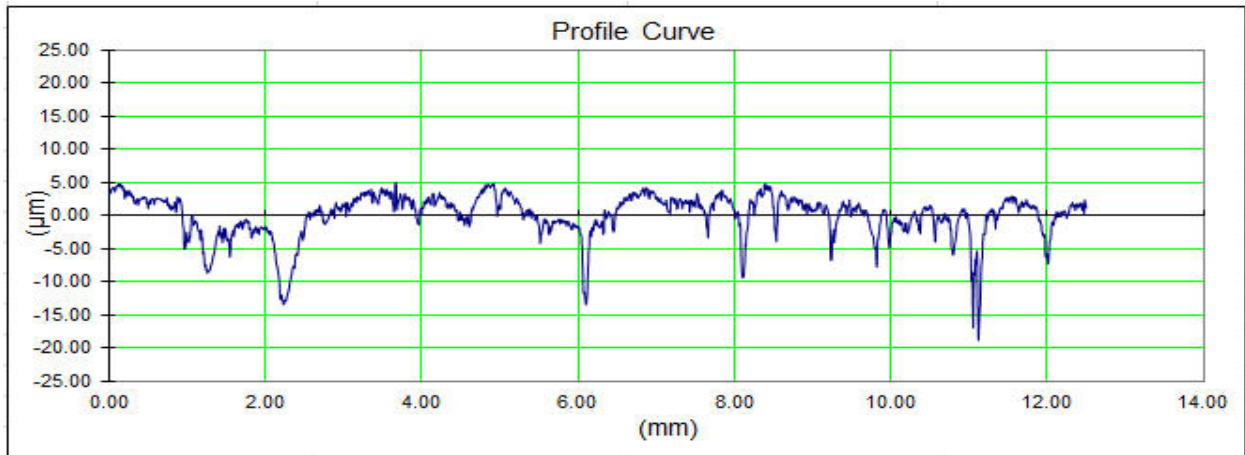


Figure 18. Scan R02 profile (exterior surface).

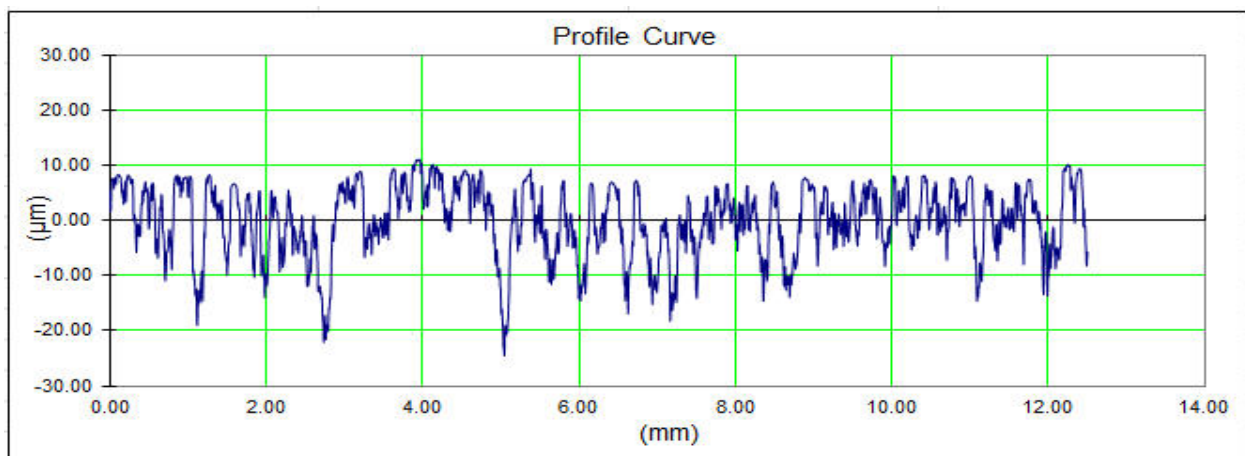


Figure 19. Scan R03 profile (interior surface).

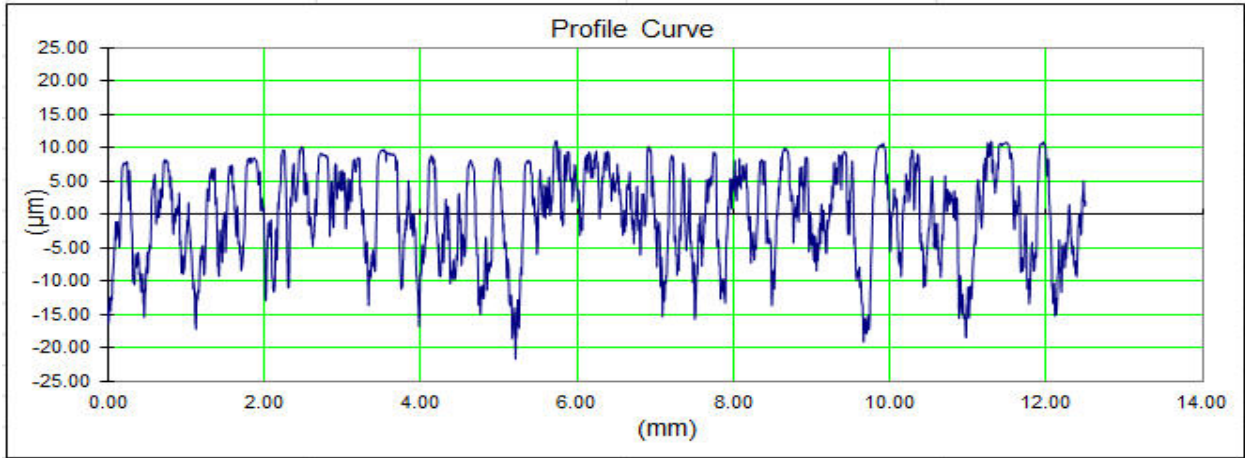


Figure 20. Scan R04 profile (interior surface).

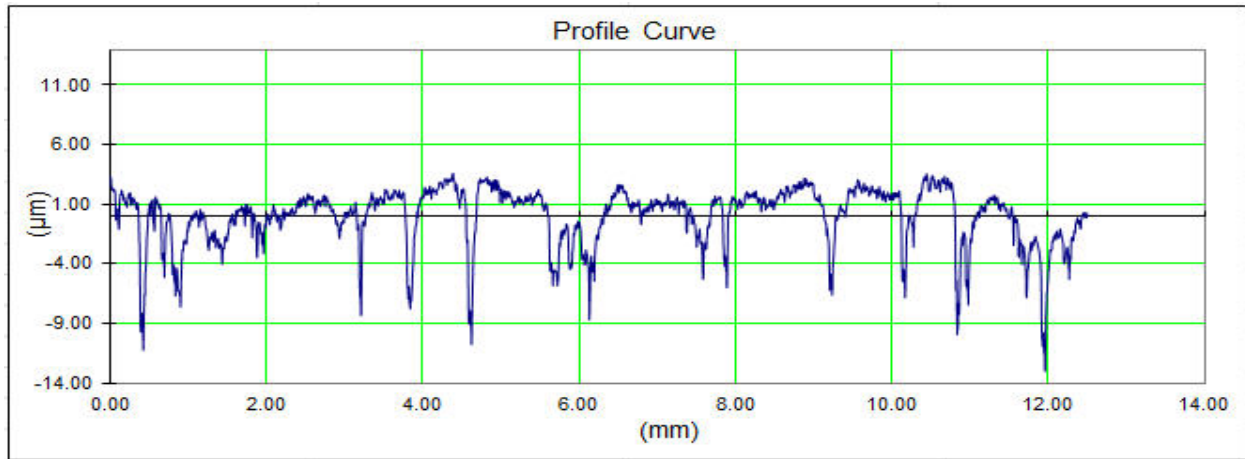


Figure 21. Scan R05 profile (exterior surface).

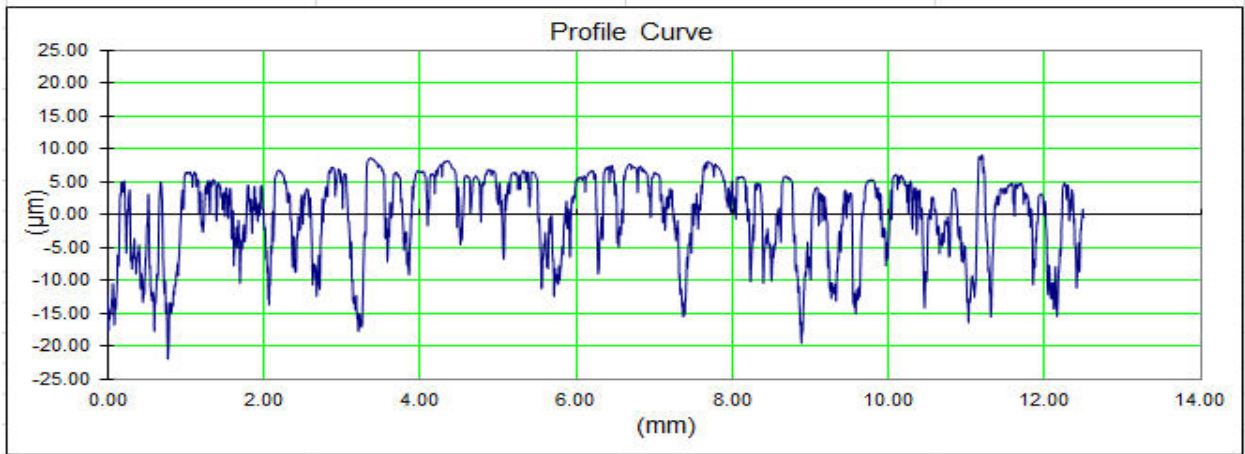


Figure 22. Scan P1_01 profile

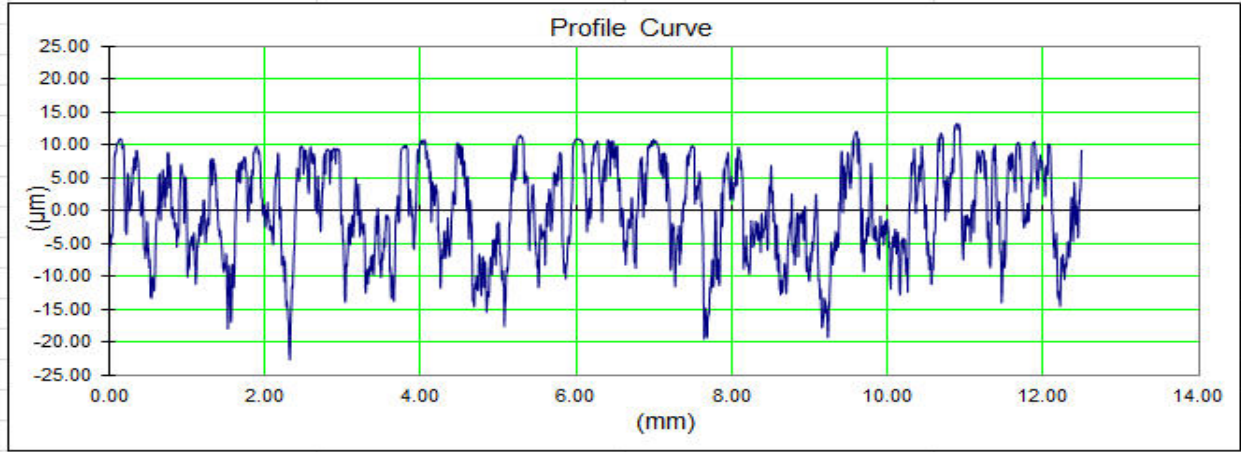


Figure 23. Scan P1_02 profile.

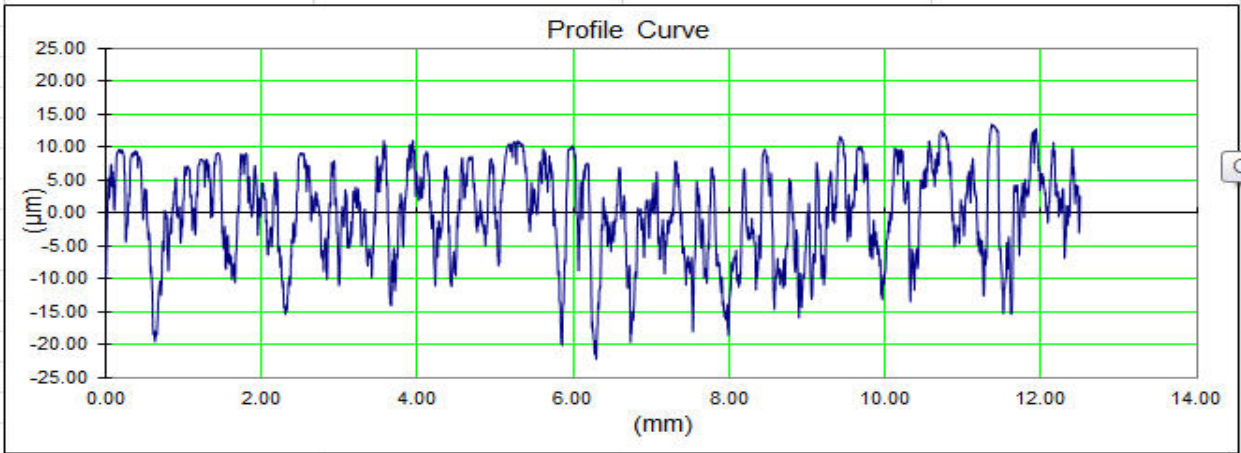


Figure 24. Scan P1_03 profile.

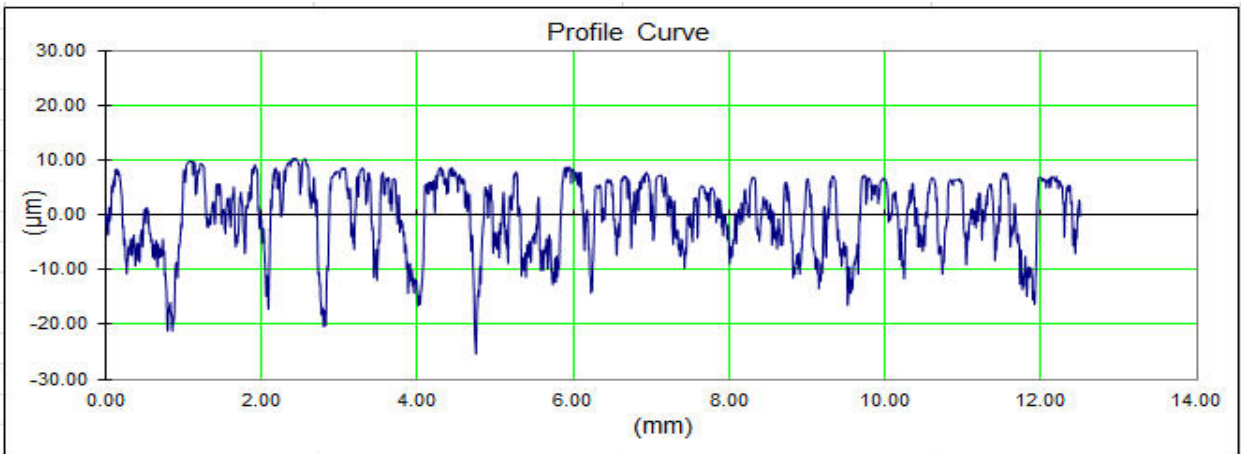


Figure 25. Scan P1_04 profile.

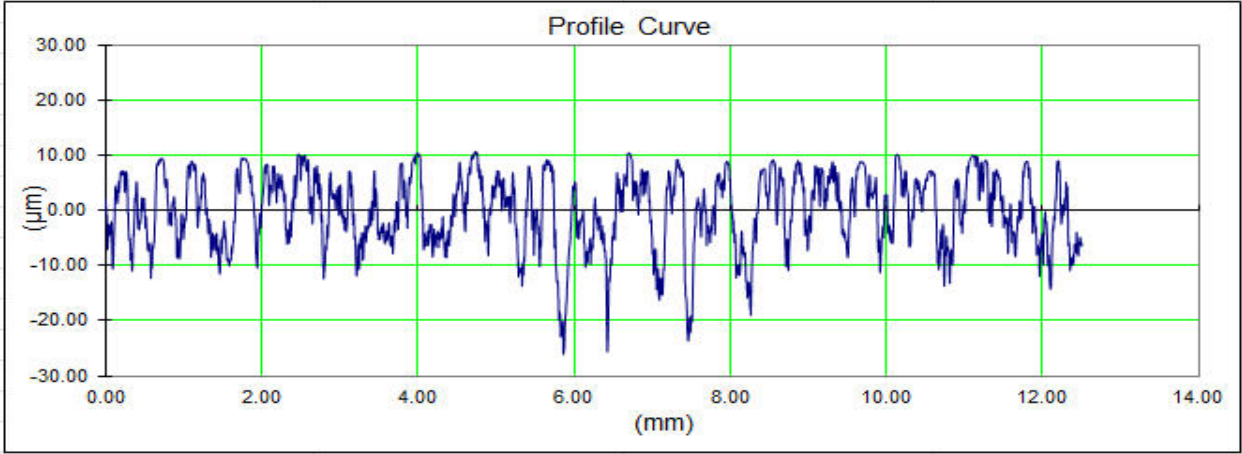


Figure 26. Scan P1_05 profile.

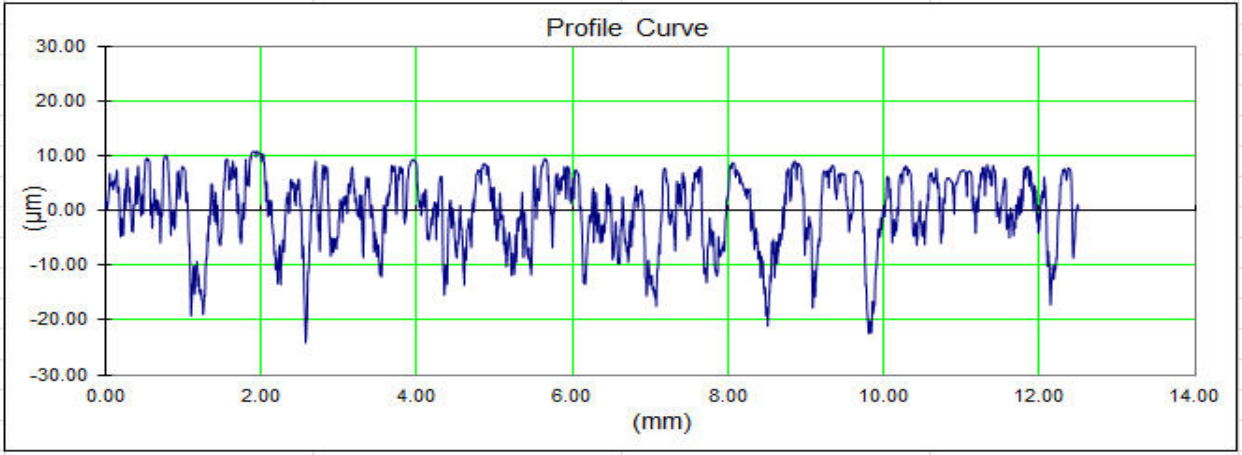


Figure 27. Scan P1_06 profile.

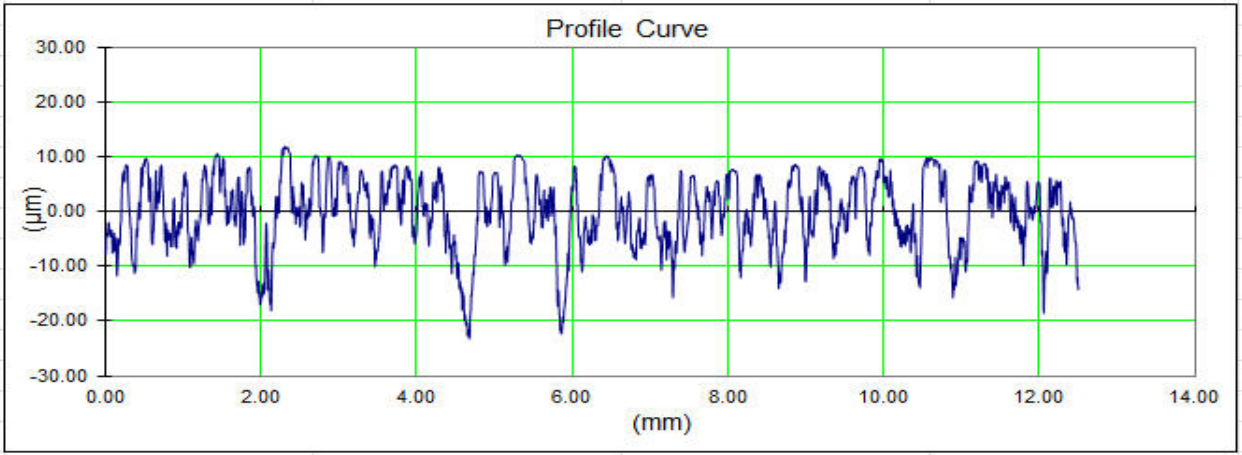


Figure 28. Scan P1_07 profile.

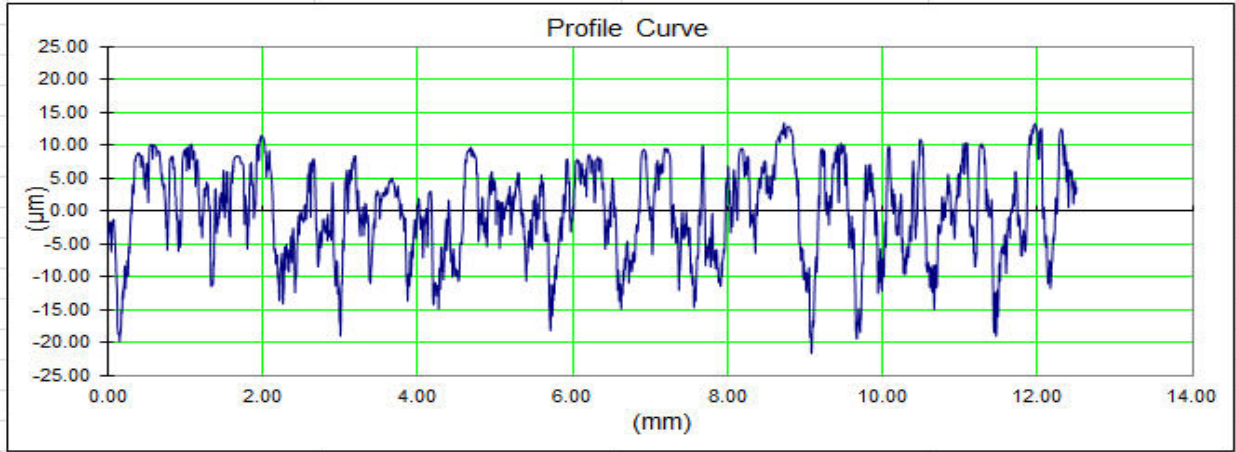


Figure 29. Scan P1_08 profile.

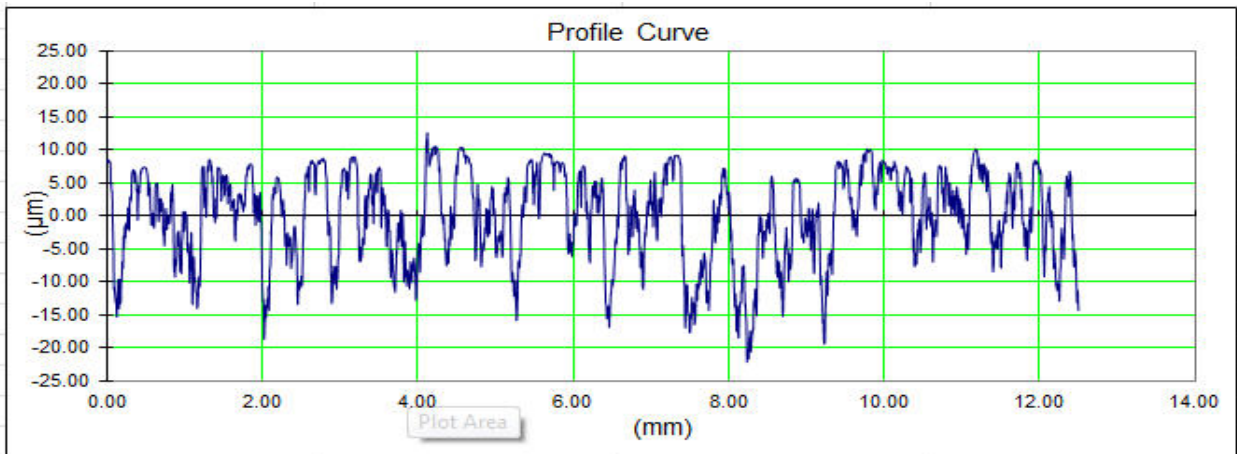


Figure 30. Scan P2_01 profile.

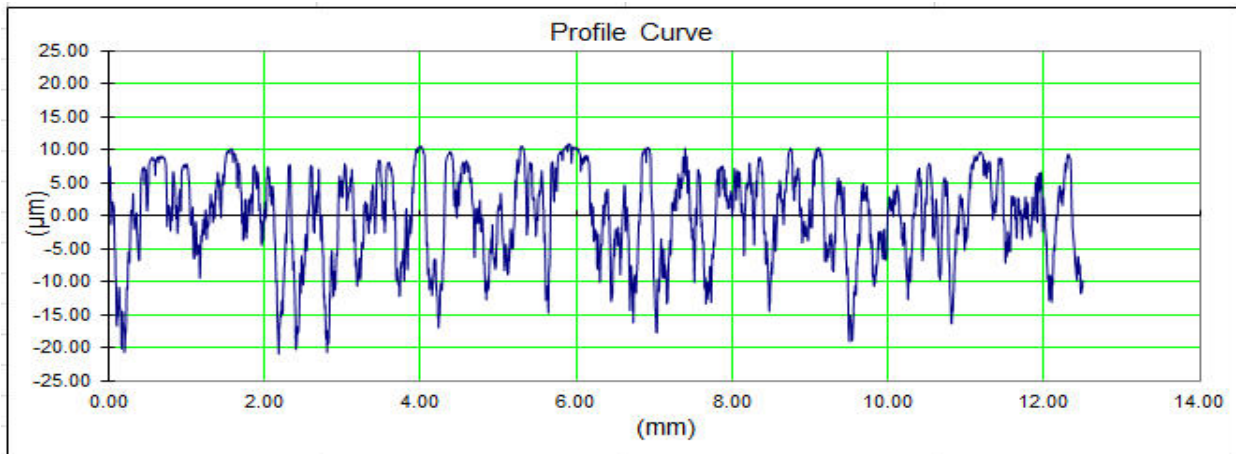


Figure 31. Scan P2_02 profile.

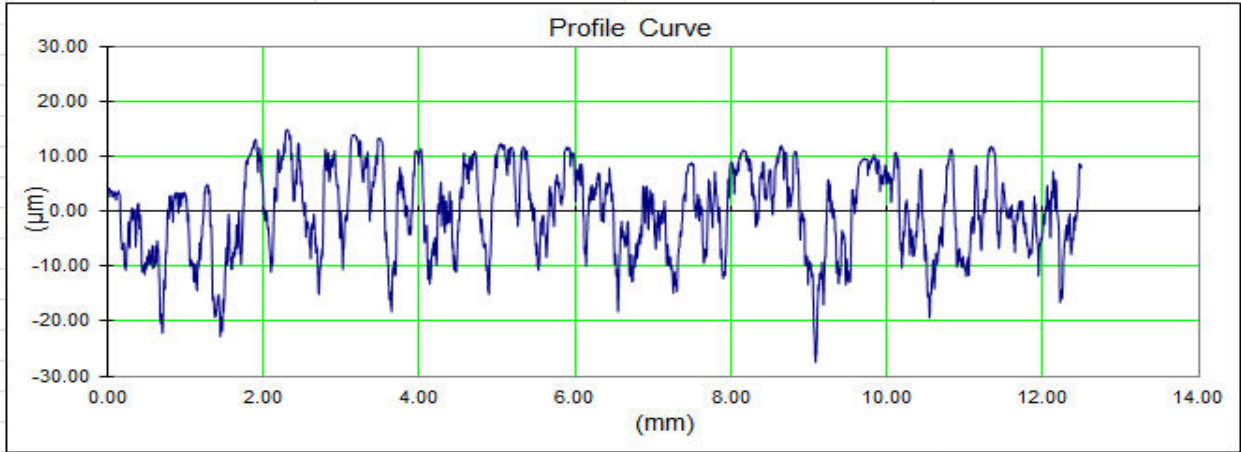


Figure 32. Scan P2_03 profile.

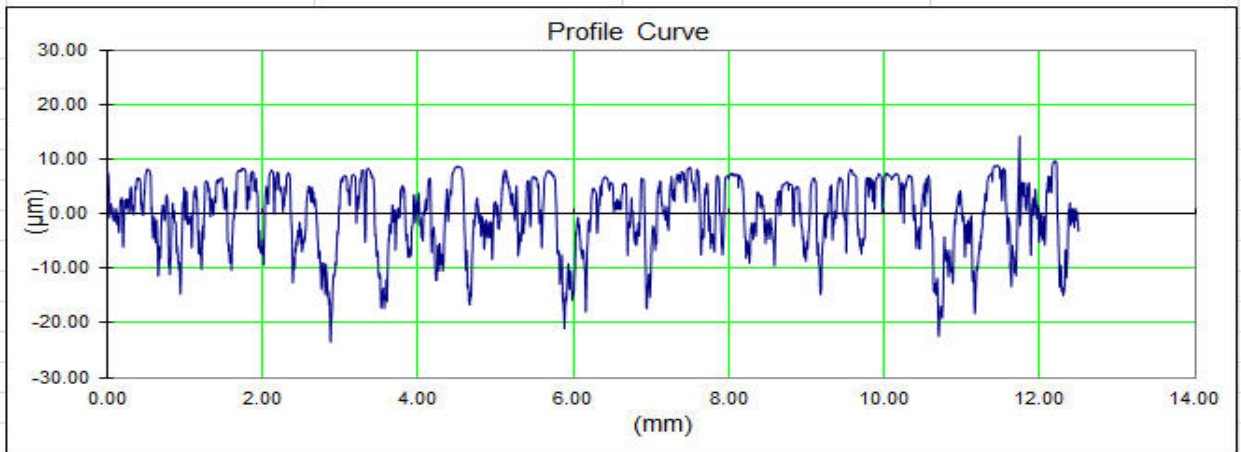


Figure 33. Scan P2_04 profile.

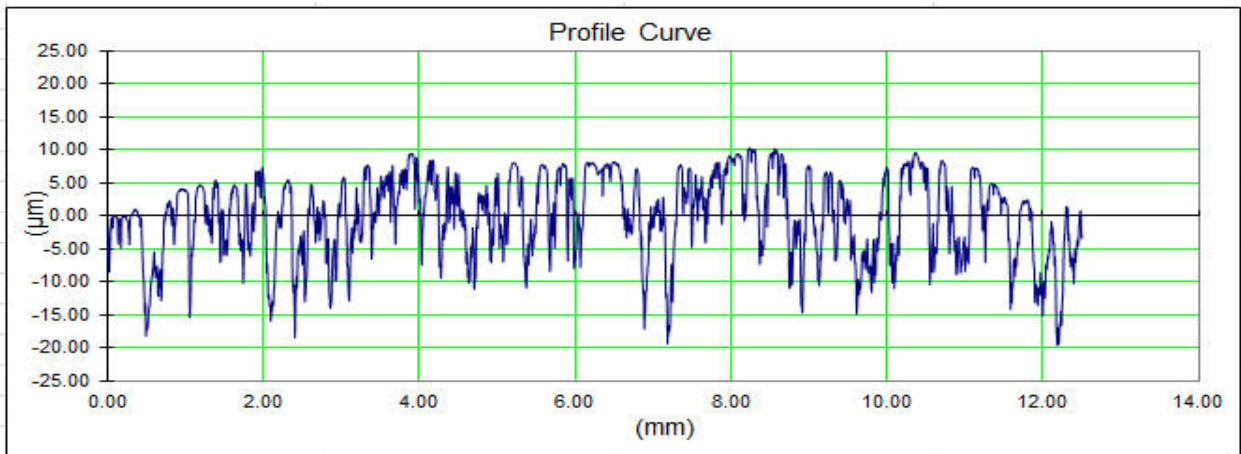


Figure 34. Scan P2_05 profile.

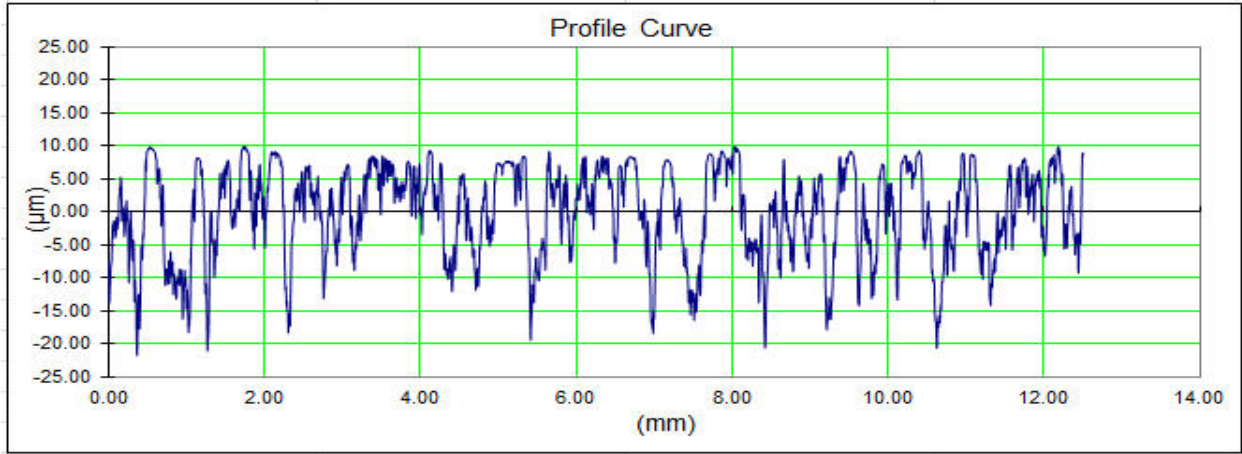


Figure 35. Scan P2_06 profile.

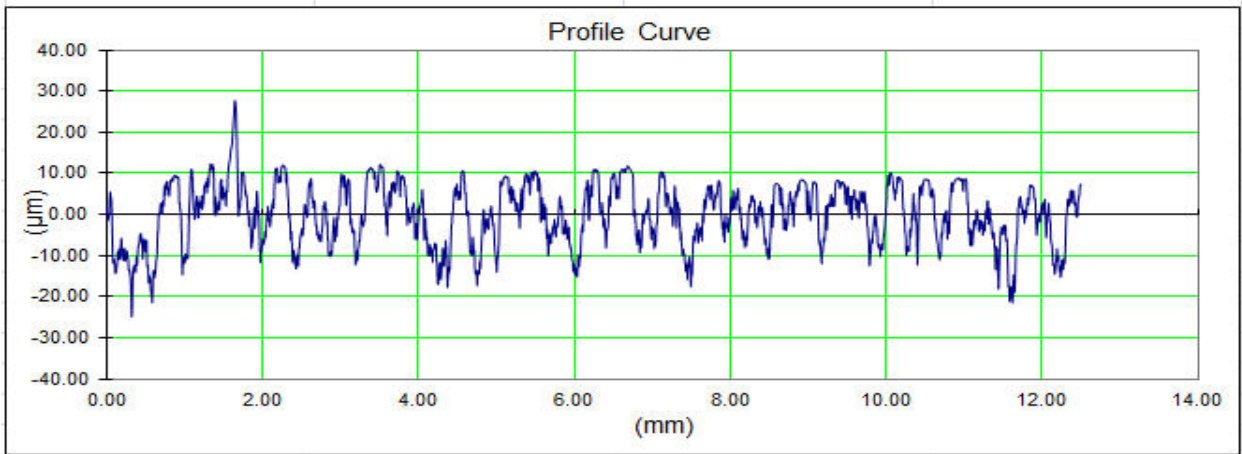


Figure 36. Scan P2_07 profile.

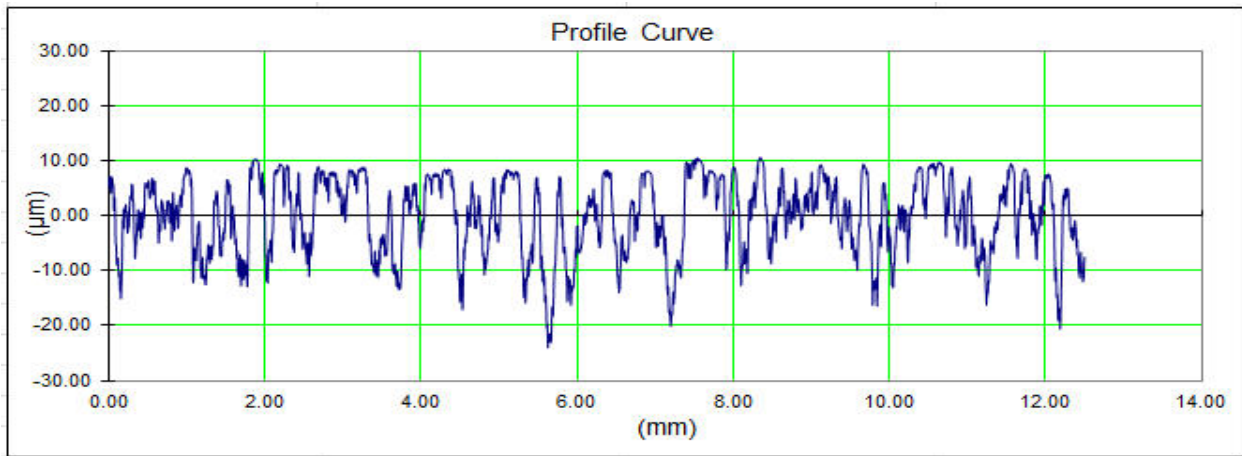


Figure 37. Scan P2_08 profile.

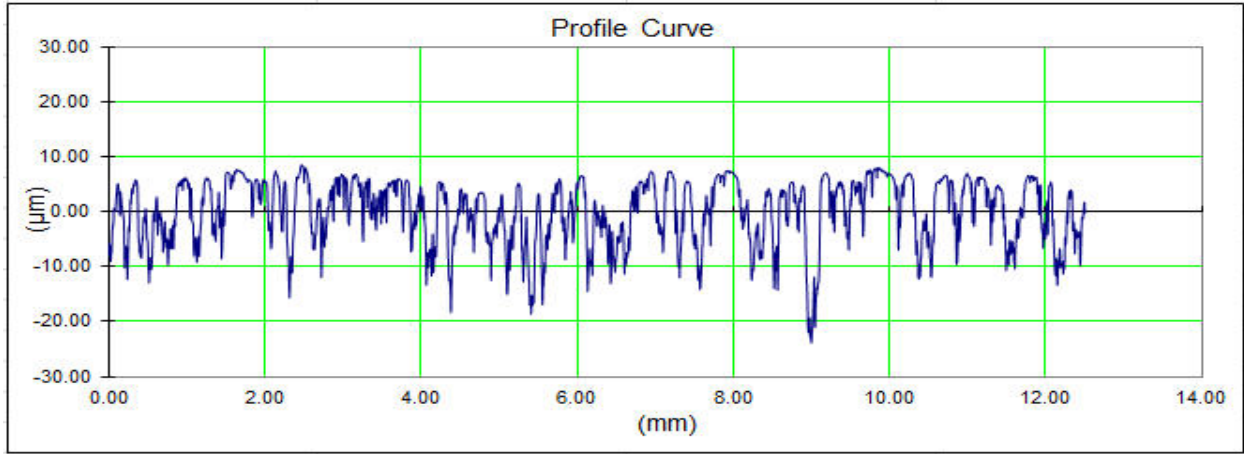


Figure 38. Scan P3_01 profile.

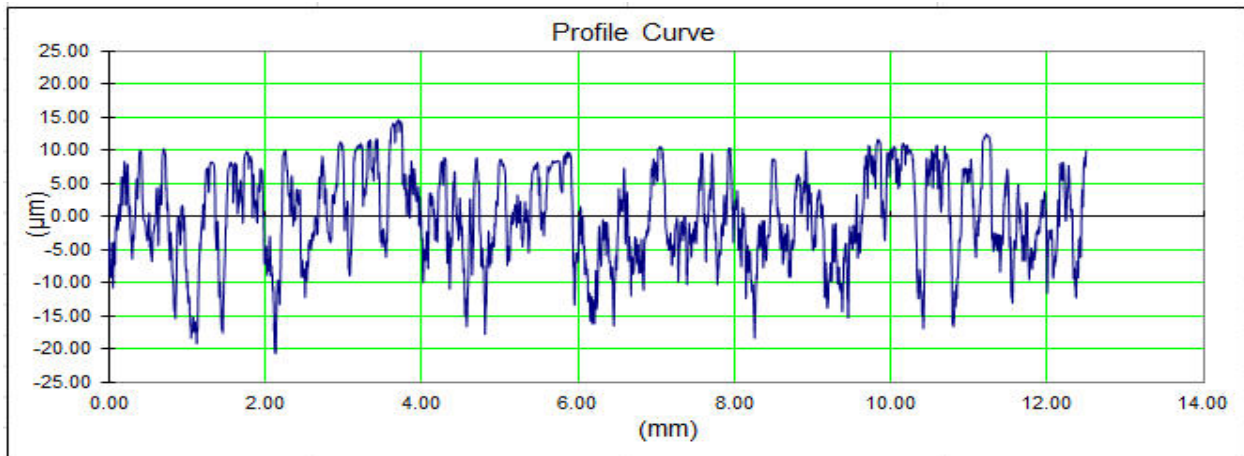


Figure 39. Scan P3_02 profile.

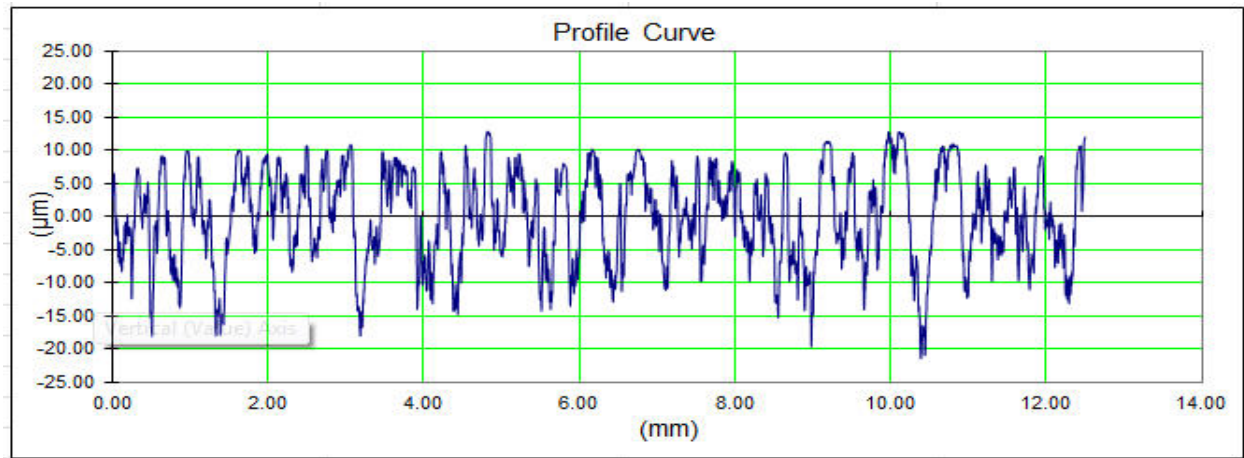


Figure 40. Scan P3_03 profile.

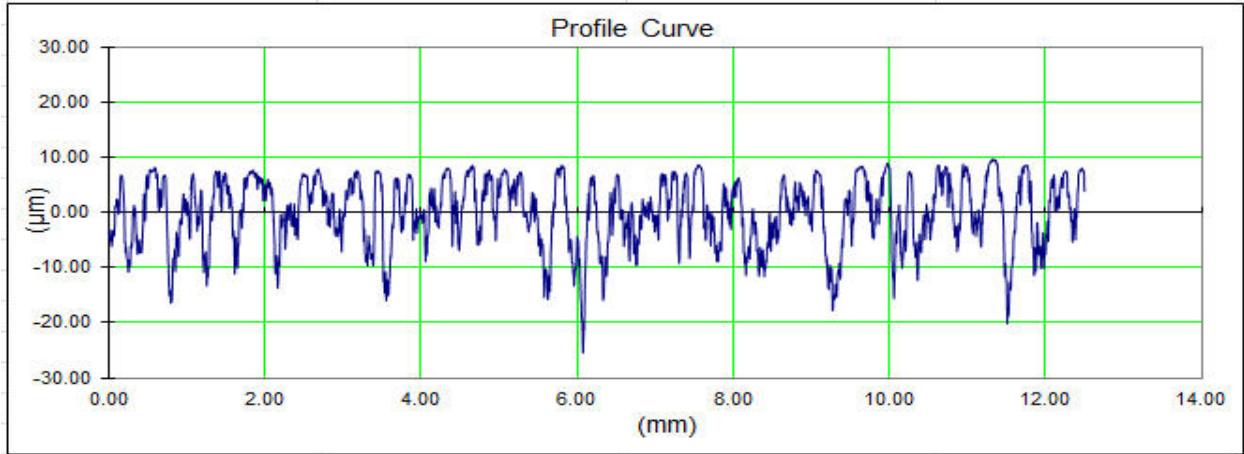


Figure 41. Scan P3_04 profile.

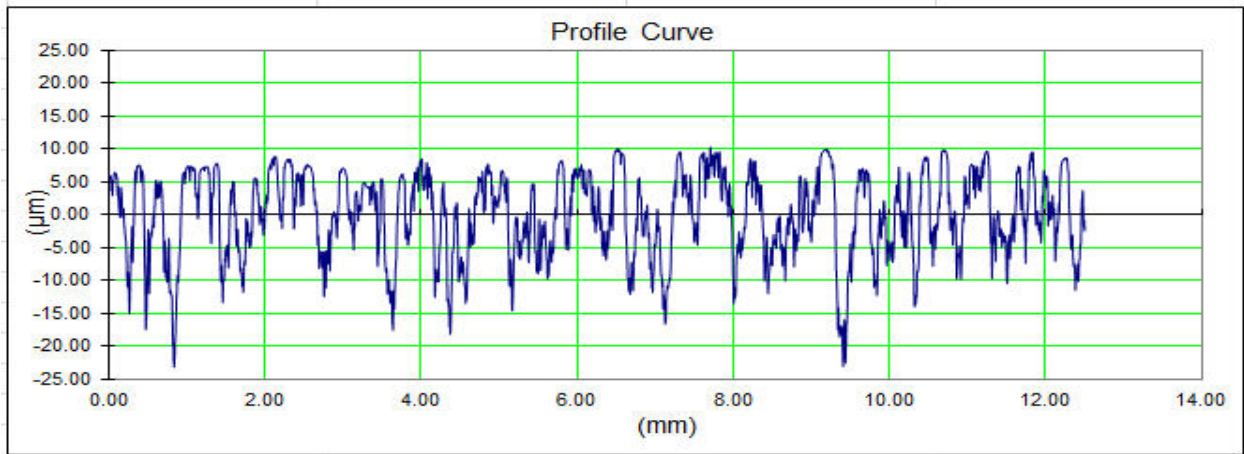


Figure 42. Scan P3_05 profile.

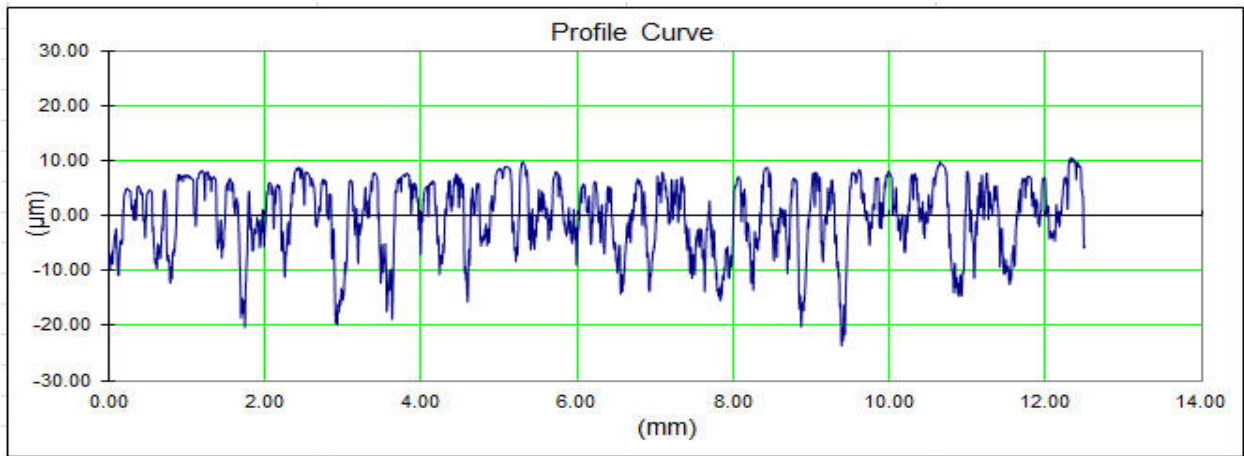


Figure 43. Scan P3_06 profile.

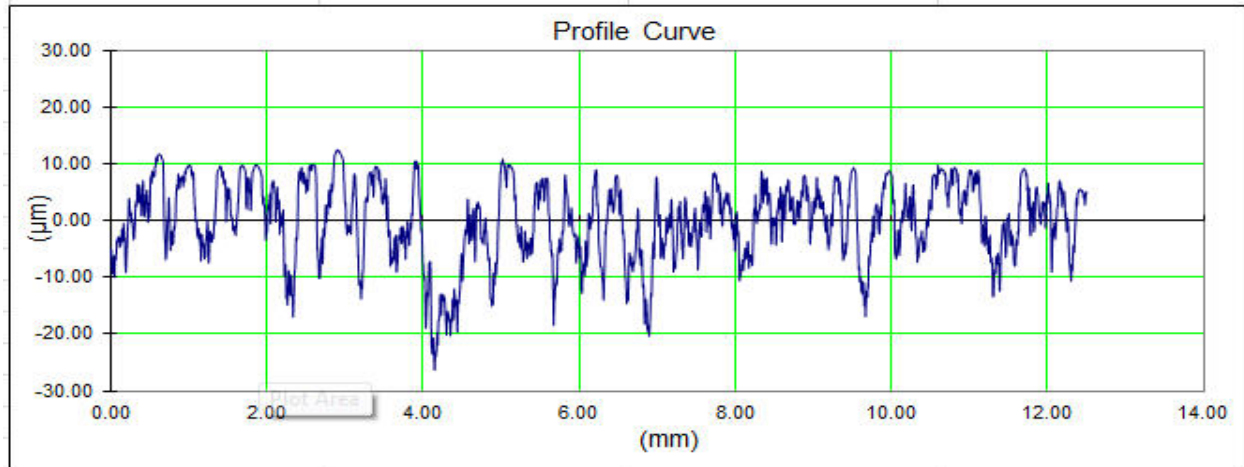


Figure 44. Scan P3_07 profile.

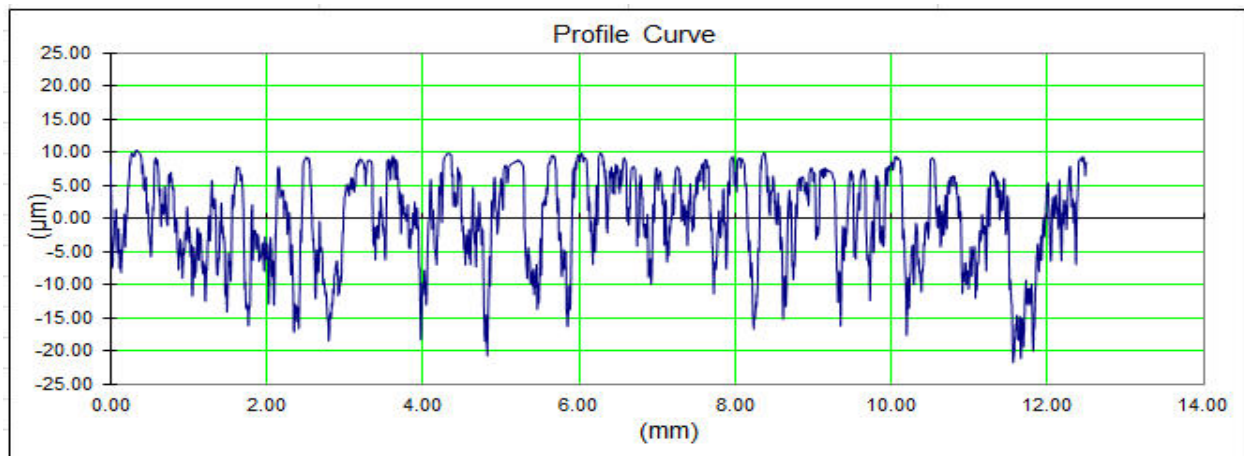


Figure 45. Scan P3_08 profile.

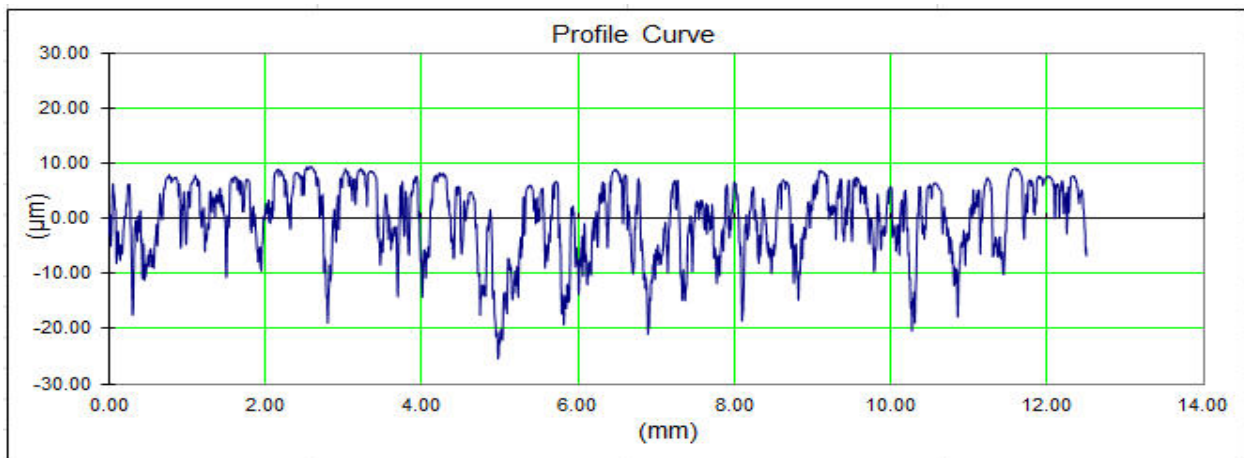


Figure 46. Scan P4_01 profile.

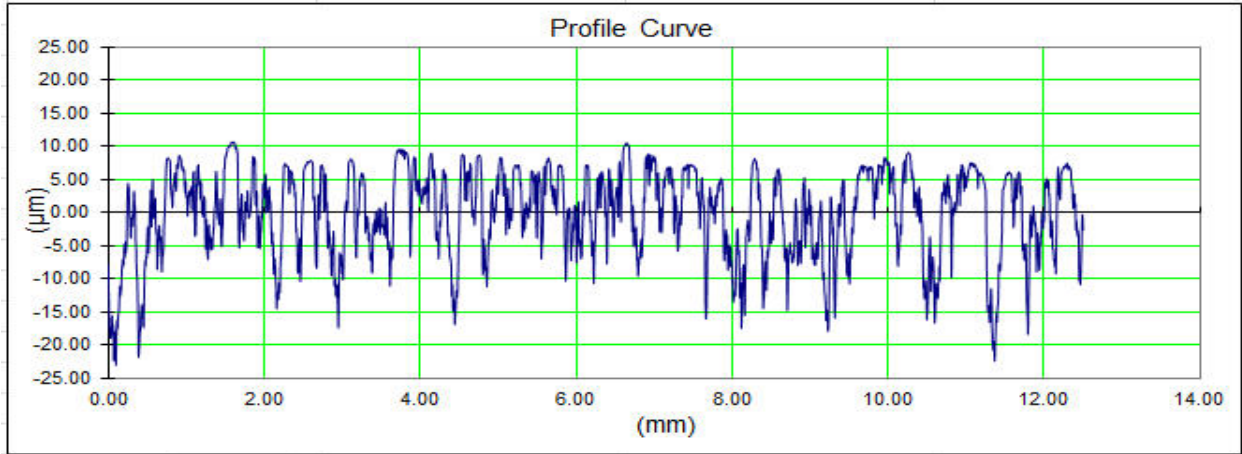


Figure 47. Scan P4_02 profile.

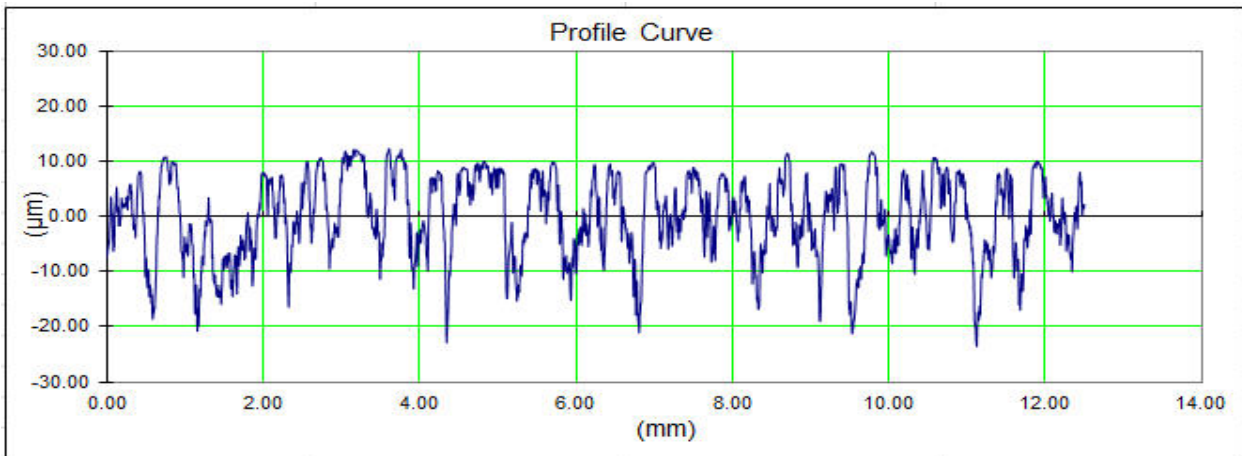


Figure 48. Scan P4_03 profile.

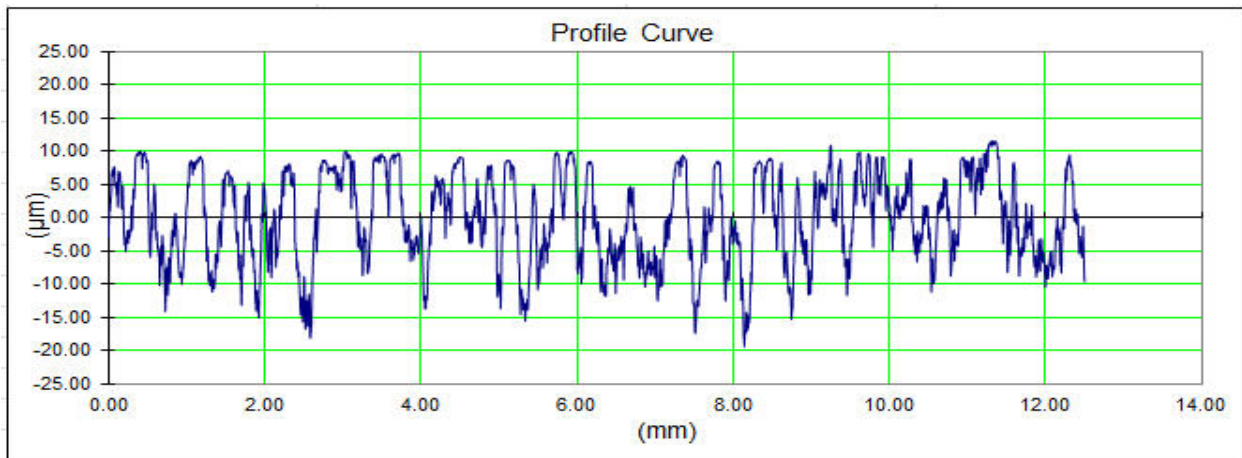


Figure 49. Scan P4_04 profile.

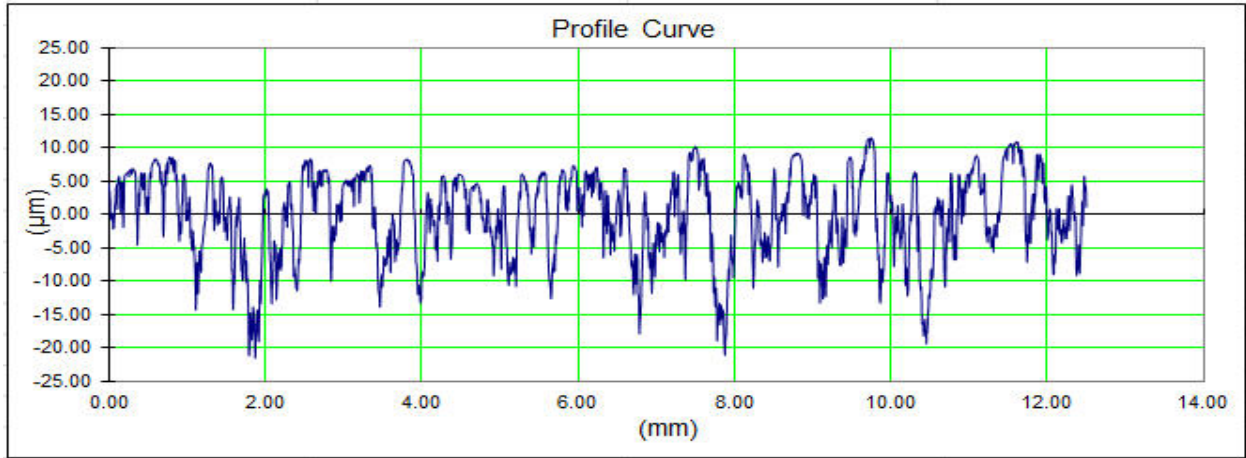


Figure 50. Scan P4_05 profile.

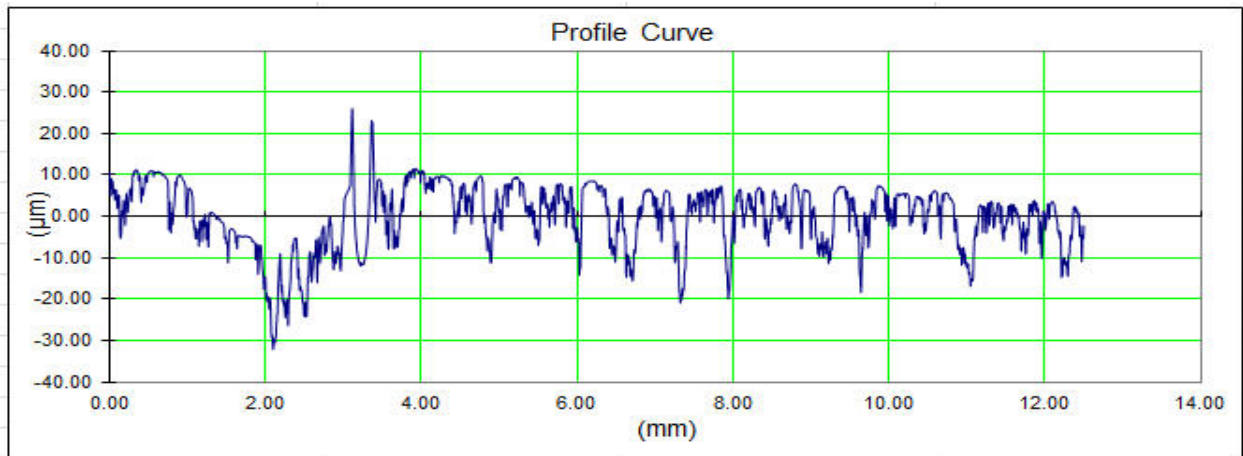


Figure 51. Scan P4_06 profile.

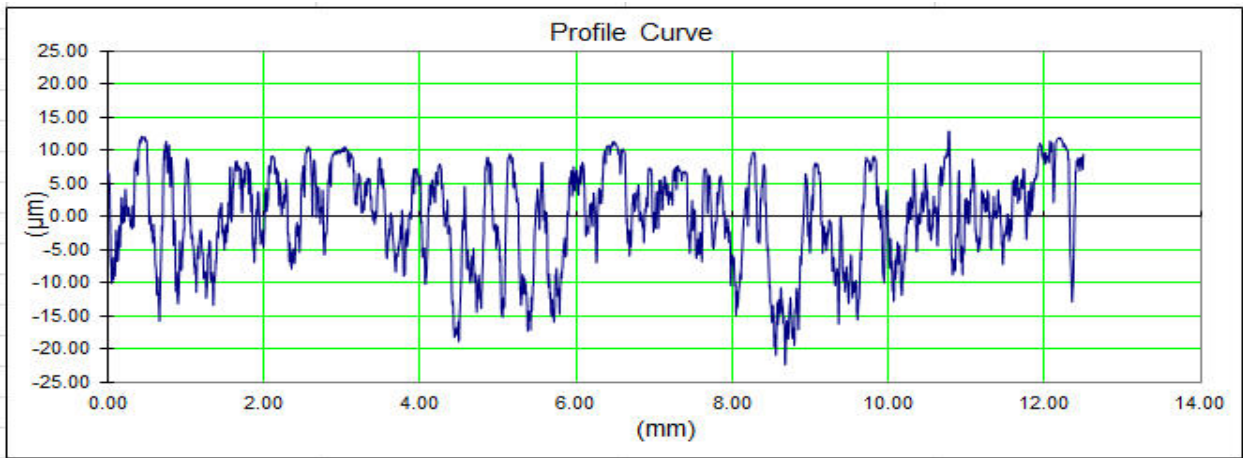


Figure 52. Scan P4_07 profile.

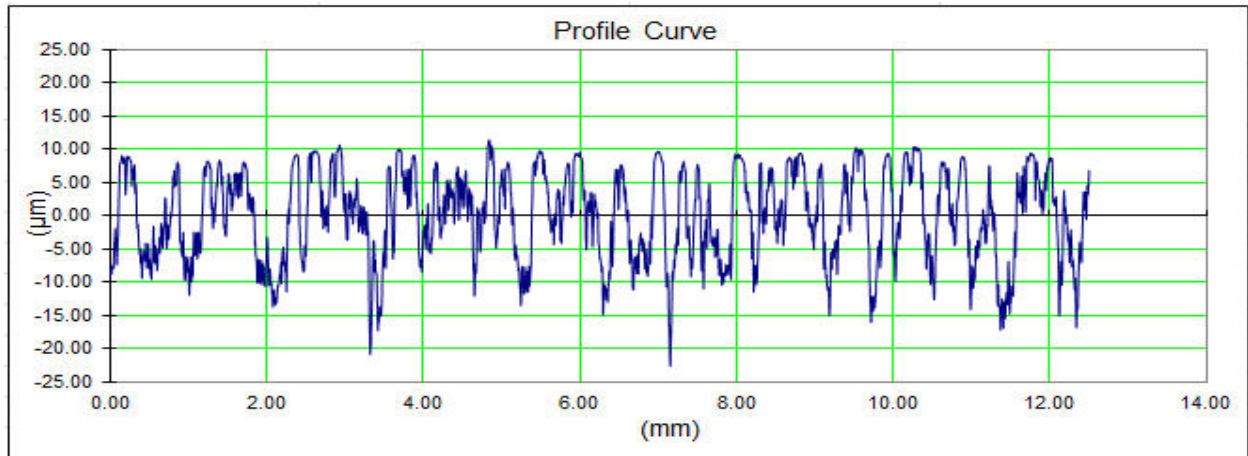


Figure 53. Scan P4_08 profile.

6.0 References

- ¹ K.T. McDonald, et al. "The MERIT High-Power Target Experiment at the CERN PS," IPAC '10, WEPE078, <http://www.hep.princeton.edu/~mcdonald/mumu/target/ipac10/wepe078.pdf>.
- ² http://www.hep.princeton.edu/~mcdonald/mumu/target/Davenne/davenne_121708.pdf.
- ³ <http://www.hep.princeton.edu/~mcdonald/mumu/target/targettrans84.pdf>, slide 29.
- ⁴ http://www.hep.princeton.edu/~mcdonald/mumu/target/graves/graves_101310.pdf.
- ⁵ http://www.hep.princeton.edu/~mcdonald/mumu/target/graves/HandySurf_011211.pdf.